A Small Signal State Space Model of Inverter-Based Microgrid Control on Single Phase AC Power Network

Sutanto Hadisupadmo, Arista Nugroho Hadiputro, and Augie Widyotriatmo, *Member, IEEE*

***Abstract*—This study describes the modeling of the inverter-based microgrid control on single-phase alternating-current (AC) network. Microgrid consists of three subsystems, which are an inverter, network, and load. Each subsystem is modeled and combined to obtain the complete model of microgrid. The control methodology examined in the system is droop-based control. Microgrid scheme designed in this study has two Distributed Generations (DGs), in which each DG is interfaced to an inverter. The inverters are connected to the load through a network. The network consists of two node/bus which are connected by a line. The inverters and loads are connected to nodes in the network. The control investigated is based on the droop control. The droop gains are designed based upon the pole placement method. Simulation is performed to show the effectiveness of the method.**

***Index Terms*—Microgrid, smart grid, distributed power generation, Power Network, alternating current, inverter, control, autonomous, renewable energy.**

I. Introduction

ENERGY demands have been significantly increased. The emergence of electricity market, fast depletion of fossil fuels, and along with environmental concerns have attracted interest in large deployment of renewable energy sources. Microgrid is a concept that integrates power generated from renewable energy sources and the grid. This offers higher flexibility, controllability, efficiency of operation, and bidirectional power flow between utility grid and the microgrid [1].

The microgrid can be operated either islanded or grid connected mode. In islanded mode, renewable energy sources supply all of load power demand. When grid connected mode, renewable energy sources are combined with the utility grid which supplies shortage power produced by the renewable energy sources. Recently, islanded mode operation is frequently developed because of some reasons associated with environmental and transmission distribution problems. Conventional power system with large power plant as power source arises environmental problem. The use of fossil fuels produces CO_2 emission and nuclear waste problem which cause greenhouse effect. Even the large hydro power plants have their own negative impacts on environment, such as potential flooding [2].

Integrating renewable DGs is the best solution to overcome shortage of power and to minimize environmental impact. However, integrating multiple DGs are not simple especially for in the scheme of AC power. It requires synchronization between multiple DGs in order to be integrated to supply loads in a grid. In DC-link voltage control [3], the power flow is controlled in DC system, therefore the synchronization becomes not necessary. Other technique uses inverter-based power flow control [4]-[10]. The inverters must be able to overcome load change with good control strategy. The frequency and voltage on the grid should be maintained within allowed limit. Other handles the issue of hybrid AC-DC microgrids [11].

In this paper, the control strategy used is the combination of feedback and feedforward control loops of power flow control in single phase AC microgrids with multiple DGs. The developed control scheme is used to connect single phase AC loads to the microgrid, which maintains desired sinusoidal load voltage waveform with required power flow and low total harmonic distortion [12]. Communication link-based control technique, such master-slave approach [13], can be used for the system where DGs are connected to common bus. Local measurement-based control technique with communication link has been proposed in [14]. Small signal state space model of a single phase AC microgrid is developed, and conventional droop control is implemented and is analyzed. The pole placement method is utilized to set the gain parameters of the controllers. Simulation results show effectiveness of the proposed method.

The paper is organized as follows. Section II provides microgrid modeling of AC power system. Section III describes the control algorithm which include power controller, voltage and current controllers, and the network model. Section IV shows simulation results. Section V draws conclusion.

Manuscript received August 6, 2015; revised August 21, 2015; accepted August 26, 2015. This work is supported in part by the Ministry of Research, Technology and Higher Education of Indonesia.

S. Hadisupadmo is with the Instrumentation and Control Research Group, Faculty of Industrial Technology, Institut Teknologi Bandung, 40132, Indonesia (email: sutanto@tf.itb.ac.id).

A. N. Hadiputro is with Instrumentation and Control Master Program, Faculty of Industrial Technology, Institut Teknologi Bandung, 40132, Indonesia (aristanugroho@ymail.com).

A. Widyotriatmo is with the Instrumentation and Control Research Group, Faculty of Industrial Technology, Institut Teknologi Bandung, 40132, Indonesia (augie@tf.itb.ac.id).

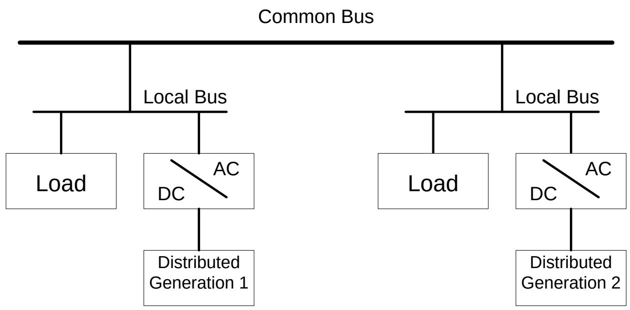

Fig. 1. Microgrid scheme.

II. MICROGRID MODELING

Fig. 1 describes the microgrid scheme in islanded mode. Two DGs with two inverters are connected to two loads through network. The inverter is used to interface a DG to load and common bus. The state equations of network and load are performed on reference frame one of the inverter. This frame reference is considered as common reference frame. All of the inverters are translated to this common reference frame using transformation technique as in [15].

Here, (D-Q) axis are common reference frame rotating at frequency ω_{com} and (d-q)i axis are i-th inverter reference frame rotating at ωi.

$$[f_{DQ}] = [T_i][f_{dq}] \tag{1}$$

$$T_i = \begin{bmatrix} \cos(\delta_i) & -\sin(\delta_i) \\ \sin(\delta_i) & \cos(\delta_i) \end{bmatrix} \tag{2}$$

where f is the quantities of electricity (current and voltage) and δ_i is angle of reference frame of i-th inverter reference frame against common reference frame.

Inverter is an electrical device that is designed to convert dc power source to ac power. The dc power source can be battery, photovoltaic, and fuel cells while ac power is standard power to run electrical equipment. Generally, inverter interfaces distributed generator to the network or load. Fig. 2 illustrates block diagram of a microgrid connected to an inverter. DG inverter uses the controller which is divided into three parts. The power controller loop sets the frequency and magnitude for inverter output voltage appropriate with droop characteristic of active and reactive power. Second and third parts are voltage and current controllers to reject high-frequency disturbance and give an adequate damping for output LC (L_f and C_f) filter [16], [17].

III. CONTROL ALGORITHM

A. Power Controller

In power controller, droop technique is usually used in synchronous generator. Synchronous generator shares the increase load with decrease frequency appropriate with governor droop characteristic. This way is applied to the inverter: if the load increases, the reference frequency decreases.

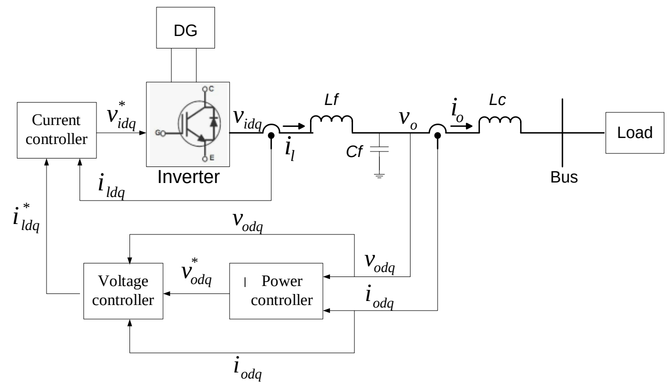

Fig. 2. Diagram block of DG inverter

Let $\tilde{p}$ dan $\tilde{q}$ be instantaneous active and reactive power are obtained from output voltage and current as:

$$\tilde{p} = v_{od} i_{od} + v_{oq} i_{oq} \tag{3}$$

$$\tilde{q} = v_{od} i_{oq} - v_{oq} i_{od} \tag{4}$$

where v and i are voltage and current respectively.

To obtain fundamental active and reactive power P and Q, the filter as in Eq. (5) is used to across instantaneous power through itself. ω_c represents the cutoff frequency of filter.

$$P = \frac{\omega_c}{s+\omega_c}\tilde{p}\,; \quad Q = \frac{\omega_c}{s+\omega_c}\tilde{q} \tag{5}$$

$$\omega = \omega_n - m_p P \tag{6}$$

Active power sharing among the inverter is obtained with bring up the droop as in Eq. (6). Frequency ω sets appropriate with droop gain (m_p). Frequency ω will decrease corresponding with active power increasing caused by power drawn of the load and ω_n represents the nominal frequency.

$$v_{od}^* = V_n - n_q Q,\; v_{oq}^* = 0 \tag{7}$$

Similarly, reactive power sharing among the inverter is obtained with bring up the droop as in Eq. (7). Voltage is set appropriate with droop gain (n_q). Voltage will decrease corresponding with reactive power increasing caused by power drawn of the load and V_n represents nominal voltage of d-axis and voltage of q-axis set by 0.

In this system, one of the inverter taken as common reference frame and first inverter taken for it. Each other variable of inverter is translated to this common reference frame use angle δ as in Eq. (8) that represents each inverter angle to common frame.

$$\delta = \int(\omega - \omega_{com}) \tag{8}$$

To simplify the notation of voltage and current in d-$q$axis, the equations are written as:

$$v_{odq}^* = [v_{od}^* \quad v_{oq}^*]^T, \quad i_{ldq} = [i_{ld} \quad i_{lq}]^T$$
$$v_{odq} = [v_{od} \quad v_{oq}]^T, \; i_{odq} = [i_{od} \quad i_{oq}]^T \tag{9}$$

By linearizing and rearrange equations above, small signal model of power controller can be written as in:

$$\begin{bmatrix} \dot{\Delta\delta} \\ \Delta P \\ \Delta Q \end{bmatrix} = A_P \begin{bmatrix} \Delta\delta \\ \Delta P \\ \Delta Q \end{bmatrix} + B_P \begin{bmatrix} \Delta i_{ldq} \\ \Delta v_{odq} \\ \Delta i_{odq} \end{bmatrix} + B_{P\omega com}[\Delta\omega_{com}]$$

$$\begin{bmatrix}\Delta\omega\\ \Delta v_{odq}^{*}\end{bmatrix}=\begin{bmatrix}C_{P\omega}\\ C_{Pv}\end{bmatrix}\begin{bmatrix}\Delta\delta\\ \Delta P\\ \Delta Q\end{bmatrix} \quad (10)$$

where

$$A_P=\begin{bmatrix}0 & -m_p & 0\\ 0 & -\omega_c & 0\\ 0 & 0 & -\omega_c\end{bmatrix} B_{P\omega com}=\begin{bmatrix}-1\\ 0\\ 0\end{bmatrix}$$

$$B_P=\begin{bmatrix}0 & 0 & 0 & 0 & 0 & 0\\ 0 & 0 & \omega_c I_{od} & \omega_c I_{oq} & \omega_c V_{od} & \omega_c V_{oq}\\ 0 & 0 & \omega_c I_{oq} & -\omega_c I_{od} & -\omega_c V_{oq} & \omega_c V_{od}\end{bmatrix}$$

$$C_{P\omega}=[0 \quad -m_p \quad 0] C_{Pv}=\begin{bmatrix}0 & 0 & -n_q\\ 0 & 0 & 0\end{bmatrix}.$$

Output from power controller is a small signal variation of reference voltage Δv_o* and frequency $\Delta\omega$.

B. Voltage Controller

Components of voltage (v_{odq}) are compared with the reference voltages ($v_{odq}ref$). These voltage errors are sent to the PI controllers, which provide the *d-q* inductor reference currents as feedback control signals and is added with *d-q* output current as feedforward for the current controller. The corresponding state equations are as follow:

$$\frac{d\phi_d}{dt}=v_{od}^{*}-v_{od}, \frac{d\phi_q}{dt}=v_{oq}^{*}-v_{oq}, \quad (11)$$

and for the *d-q* inductor reference currents are:

$$i_{ld}^{*}=Fi_{od}-\omega_n C_f v_{oq}+K_{pv}(v_{od}^{*}-v_{od})+K_{iv}\phi_d \quad (12)$$

$$i_{lq}^{*}=Fi_{oq}+\omega_n C_f v_{od}+K_{pv}(v_{oq}^{*}-v_{oq})+K_{iv}\phi_q \quad (13)$$

where$F$, K_{pv} and K_{iv} are positive constants.

Equations (14) and (15) represent linearizing small signal state space of the voltage controller.

$$[\Delta\dot{\phi}_{dq}]=[0][\Delta\phi_{dq}]+B_{V1}[\Delta v_{odq}^{*}]+B_{V2}\begin{bmatrix}\Delta i_{ldq}\\ \Delta v_{odq}\\ \Delta i_{odq}\end{bmatrix} \quad (14)$$

$$[\Delta i_{ldq}^{*}]=C_V[\Delta\phi_{dq}]+D_{V1}[\Delta v_{odq}^{*}]+D_{V2}\begin{bmatrix}\Delta i_{ldq}\\ \Delta v_{odq}\\ \Delta i_{odq}\end{bmatrix} \quad (15)$$

where

$$\Delta\phi_{dq}=[\Delta\phi_d \quad \Delta\phi_q]^T,$$

$$B_{V1}=\begin{bmatrix}1 & 0\\ 0 & 1\end{bmatrix}, B_{V2}=\begin{bmatrix}0 & 0 & -1 & 0 & 0 & 0\\ 0 & 0 & 0 & -1 & 0 & 0\end{bmatrix},$$

$$[\Delta i_{ldq}^{*}]=C_V[\Delta\phi_{dq}]+D_{V1}[\Delta v_{odq}^{*}]+D_{V2}\begin{bmatrix}\Delta i_{ldq}\\ \Delta v_{odq}\\ \Delta i_{odq}\end{bmatrix},$$

$$C_V=\begin{bmatrix}K_{iv} & 0\\ 0 & K_{iv}\end{bmatrix}, D_{V1}=\begin{bmatrix}K_{pv} & 0\\ 0 & K_{pv}\end{bmatrix},$$

$$D_{V2}=\begin{bmatrix}0 & 0 & -K_{pv} & -\omega_n C_f & F & 0\\ 0 & 0 & \omega_n C_f & -K_{pv} & 0 & F\end{bmatrix}.$$

C. Current Controller

Components of inductor current (i_{ldq}) are compared with the reference current (i_{ldq}^{*}). These current errors are sent to the PI controllers, which provide the *d-q* reference voltage as feedback control signals for the inverter. The corresponding state equations as follow:

$$\frac{d\gamma_d}{dt}=i_{ld}^{*}-i_{ld}, \quad \frac{d\gamma_q}{dt}=i_{lq}^{*}-i_{lq} \quad (16)$$

and for the *d-q* reference voltages of the inverter are

$$v_{id}^{*}=-\omega_n L_f i_{lq}+K_{pc}(i_{ld}^{*}-i_{ld})+K_{ic}\gamma_d \quad (17)$$

$$v_{iq}^{*}=\omega_n L_f i_{ld}+K_{pc}(i_{lq}^{*}-i_{lq})+K_{ic}\gamma_q \quad (18)$$

Eqs. (19) and (20) represent linearizing small signal state space of the current controller.

$$[\Delta\dot{\gamma}_{dq}]=[0][\Delta\gamma_{dq}]+B_{C1}[\Delta i_{ldq}^{*}]+B_{C2}\begin{bmatrix}\Delta i_{ldq}\\ \Delta v_{odq}\\ \Delta i_{odq}\end{bmatrix} \quad (19)$$

$$[\Delta v_{idq}^{*}]=C_C[\Delta\gamma_{dq}]+D_{C1}[\Delta i_{ldq}^{*}]+D_{C2}\begin{bmatrix}\Delta i_{ldq}\\ \Delta v_{odq}\\ \Delta i_{odq}\end{bmatrix} \quad (20)$$

where

$$B_{C1}=\begin{bmatrix}1 & 0\\ 0 & 1\end{bmatrix}, B_{C2}=\begin{bmatrix}-1 & 0 & 0 & 0 & 0 & 0\\ 0 & -1 & 0 & 0 & 0 & 0\end{bmatrix},$$

$$[\Delta v_{idq}^{*}]=C_C[\Delta\gamma_{dq}]+D_{C1}[\Delta i_{ldq}^{*}]+D_{C2}\begin{bmatrix}\Delta i_{ldq}\\ \Delta v_{odq}\\ \Delta i_{odq}\end{bmatrix},$$

$$C_C=\begin{bmatrix}K_{ic} & 0\\ 0 & K_{ic}\end{bmatrix}, D_{C1}=\begin{bmatrix}K_{pc} & 0\\ 0 & K_{pc}\end{bmatrix},$$

$$D_{C2}=\begin{bmatrix}-K_{pc} & -\omega_n L_f & 0 & 0 & 0 & 0\\ \omega_n L_f & -K_{pc} & 0 & 0 & 0 & 0\end{bmatrix}.$$

D. LC Filter Output

State equations of LC filter output can be represented as follow:

$$\frac{di_{ld}}{dt}=\frac{-r_f}{L_f}i_{ld}+\omega i_{lq}+\frac{1}{L_f}v_{id}-\frac{1}{L_f}v_{od} \quad (21)$$

$$\frac{di_{lq}}{dt}=\frac{-r_f}{L_f}i_{lq}-\omega i_{ld}+\frac{1}{L_f}v_{iq}-\frac{1}{L_f}v_{oq} \quad (22)$$

$$\frac{dv_{od}}{dt}=\omega v_{oq}+\frac{1}{C_f}i_{ld}-\frac{1}{C_f}i_{od} \quad (23)$$

$$\frac{dv_{oq}}{dt}=-\omega v_{od}+\frac{1}{C_f}i_{lq}-\frac{1}{C_f}i_{oq} \quad (24)$$

$$\frac{di_{od}}{dt}=\frac{-r_c}{L_c}i_{od}+\omega i_{oq}+\frac{1}{L_c}v_{od}-\frac{1}{L_c}v_{bd} \quad (25)$$

$$\frac{di_{oq}}{dt}=\frac{-r_c}{L_c}i_{oq}-\omega i_{od}+\frac{1}{L_c}v_{oq}-\frac{1}{L_c}v_{bq} \quad (26)$$

By linearizing, Eq. (27) represents small signal state space of the LC filter output.

$$\begin{bmatrix}\Delta\dot{i}_{ldq}\\ \Delta\dot{v}_{odq}\\ \Delta\dot{i}_{odq}\end{bmatrix}=A_{LCL}\begin{bmatrix}\Delta i_{ldq}\\ \Delta v_{odq}\\ \Delta i_{odq}\end{bmatrix}+B_{LCL1}[\Delta v_{idq}] + B_{LCL2}[\Delta v_{bdq}]+B_{LCL3}[\Delta\omega] \quad (27)$$

where

$$A_{LCL}=\begin{bmatrix}\frac{-r_f}{L_f} & \omega_0 & \frac{-1}{L_f} & 0 & 0 & 0\\ -\omega_0 & \frac{-r_f}{L_f} & 0 & \frac{-1}{L_f} & 0 & 0\\ \frac{1}{C_f} & 0 & 0 & \omega_0 & \frac{-1}{C_f} & 0\\ 0 & \frac{1}{C_f} & -\omega_0 & 0 & 0 & \frac{-1}{C_f}\\ 0 & 0 & \frac{1}{L_c} & 0 & \frac{-r_c}{L_c} & \omega_0\\ 0 & 0 & 0 & \frac{1}{L_c} & -\omega_0 & \frac{-r_c}{L_c}\end{bmatrix},$$

$$B_{LCL1}=\begin{bmatrix}\frac{1}{L_f} & 0\\ 0 & \frac{1}{L_f}\\ 0 & 0\\ 0 & 0\\ 0 & 0\\ 0 & 0\end{bmatrix}\quad B_{LCL2}=\begin{bmatrix}0 & 0\\ 0 & 0\\ 0 & 0\\ 0 & 0\\ \frac{-1}{L_c} & 0\\ 0 & \frac{-1}{L_c}\end{bmatrix},$$

$$B_{LCL3}=[I_{lq}\quad -I_{ld}\quad V_{oq}\quad -V_{od}\quad I_{oq}\quad -I_{od}]^T.$$

E. Complete Model of an Inverter

State space model of the power controller, voltage controller, current controller, and LC filter output are used to obtain the complete model of an inverter as in Eq. (28)

$$\begin{gathered}[\Delta\dot{x}_{\text{inv}i}]=A_{\text{INVi}}[\Delta x_{\text{inv}i}]+B_{\text{INVi}}[\Delta v_{bDQi}]\\ +B_{i\omega com}[\Delta\omega_{com}]\\ \begin{bmatrix}\Delta\omega_i\\ \Delta i_{oDQi}\end{bmatrix}=\begin{bmatrix}C_{\text{INV}\omega\text{i}}\\ C_{\text{INVci}}\end{bmatrix}[\Delta x_{\text{inv}i}],\end{gathered}\tag{28}$$

where

$$\Delta x_{\text{inv}i}=[\Delta\delta_i\quad \Delta P_i\quad \Delta Q_i\quad \Delta\phi_{dqi}\quad \Delta\gamma_{dqi}\quad \Delta i_{ldqi}\quad \Delta v_{odqi}\quad \Delta i_{odqi}]^T$$

and the rest of terms are shown at the bottom of the page.

F. Network Model

This study uses a network with two nodes connected with one line. In common reference frame, state equations of line current which connected at *j*-node and *k*-node are:

$$\frac{di_{lineDi}}{dt}=\frac{-r_{linei}}{L_{linei}}i_{lineDi}+\omega i_{lineQi}+\frac{1}{L_{linei}}v_{bDj}-\frac{1}{L_{linei}}v_{bDk}\tag{29}$$

$$\frac{di_{lineQi}}{dt}=\frac{-r_{linei}}{L_{linei}}i_{lineQi}-\omega i_{lineDi}+\frac{1}{L_{linei}}v_{bQj}-\frac{1}{L_{linei}}v_{bQk}\tag{30}$$

So, the small signal state space model of the network is:

$$[\Delta\dot{i}_{\text{lineDQ}}]=A_{\text{NET}}[\Delta i_{\text{lineDQ}}]+B_{1\text{NET}}[\Delta v_{bDQ}]+B_{2NET}\Delta\omega\tag{31}$$

where

$$A_{\text{NET}}=[A_{\text{NET 1}}]_{2\times 2},$$

$$B_{1\text{NET}}=[B_{1\text{NET 1}}]_{2\times 4},$$

$$B_{2\text{NET}}=[B_{2\text{NET 1}}]_{2\times 1},$$

$$A_{\text{NETi}}=\begin{bmatrix}\frac{-r_{linei}}{L_{linei}} & \omega_0\\ -\omega_0 & \frac{-r_{linei}}{L_{linei}}\end{bmatrix}B_{2\text{NET}}=\begin{bmatrix}I_{\text{lineQi}}\\ -I_{\text{lineDi}}\end{bmatrix},$$

$$B_{1\text{NETi}}=\begin{bmatrix}\frac{1}{L_{linei}} & 0 & \frac{-1}{L_{linei}} & 0\\ 0 & \frac{1}{L_{linei}} & 0 & \frac{-1}{L_{linei}}\end{bmatrix}_{2\times 4}.$$

G. Load model

This study uses two RL load for the load of microgrid. These loads are connected at each node. The state equations of the load connected at *i*-node is:

$$\frac{di_{loadDi}}{dt}=\frac{-r_{loadi}}{L_{loadi}}i_{loadDi}+\omega i_{loadQi}+\frac{1}{L_{loadi}}v_{bDi},\tag{32}$$

$$\frac{di_{loadQi}}{dt}=\frac{-r_{loadi}}{L_{loadi}}i_{loadQi}-\omega i_{loadDi}+\frac{1}{L_{loadi}}v_{bQi}.\tag{33}$$

So, the small signal state space model of the load as in:

$$[\Delta\dot{i}_{\text{loadDQ}}]=A_{\text{load}}[\Delta i_{\text{loadDQ}}]+B_{1\text{LOAD}}[\Delta v_{bDQ}]+B_{2\text{LOAD}}\Delta\omega\tag{34}$$

where

$$A_{\text{load}}=\begin{bmatrix}A_{\text{load 1}} & 0\\ 0 & A_{\text{load 2}}\end{bmatrix}_{4\times 4},$$

The linked image cannot be displayed. The file may have been moved, renamed, or deleted. Verify that the link points to the correct file and location.

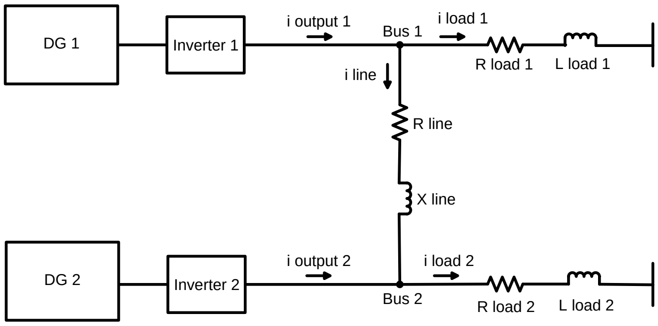

Fig. 3. Two-DGs-two-Loads microgrid network.

$$B_{1\mathrm{LOAD\ i}} = \begin{bmatrix} \frac{1}{L_{loadi}} & 0 & 0 & 0 \\ 0 & \frac{1}{L_{loadi}} & 0 & 0 \\ 0 & 0 & \frac{1}{L_{loadi}} & 0 \\ 0 & 0 & 0 & \frac{1}{L_{loadi}} \end{bmatrix}_{4\times4},$$

$$B_{1\mathrm{LOAD}} = \begin{bmatrix} B_{1\mathrm{LOAD\ 1}} \\ B_{1\mathrm{LOAD\ 2}} \end{bmatrix}_{4\times4},$$

$$B_{2\mathrm{LOAD}} = \begin{bmatrix} B_{2\mathrm{LOAD\ 1}} \\ B_{2\mathrm{LOAD\ 2}} \end{bmatrix}_{4\times1},$$

$$A_{\mathrm{load\ i}} = \begin{bmatrix} \frac{-r_{loadi}}{L_{loadi}} & \omega_0 \\ -\omega_0 & \frac{-r_{loadi}}{L_{loadi}} \end{bmatrix} B_{2\mathrm{LOAD\ i}} = \begin{bmatrix} I_{\mathrm{loadQi}} \\ -I_{\mathrm{loadDi}} \end{bmatrix}.$$

H. Complete Model of Microgrid

The complete microgrid small signal state space model and the system state matrix can be obtained by combining individual subsystem.

$$\begin{bmatrix} \Delta \dot{x}_{INV} \\ \Delta \dot{i}_{lineDQ} \\ \Delta \dot{i}_{loadDQ} \end{bmatrix} = A_{mg} \begin{bmatrix} \Delta x_{INV} \\ \Delta i_{lineDQ} \\ \Delta i_{loadDQ} \end{bmatrix}. \qquad (35)$$

Where A_{mg} is as in the bottom of the page.

IV. Simulation Results

In this study, two-DGs-two-Loads microgrid network is investigated. Fig. 3. shows the network configuration. To consider stability of the microgrid system, it can be done by looking for eigenvalues of the system matrix. Fig. 4 shows complete eigenvalues of the system. All of the complex eigenvalues have negative values which represent the system is stable focus towards zero. Real component of eigenvalue gives damping and imaginer component gives oscillation frequency. From Fig. 5, it can be shown the real part of eigenvalues have negative value which shows the system is damped. If real part of eigenvalues have positive value, it conducts increasing of oscillation.

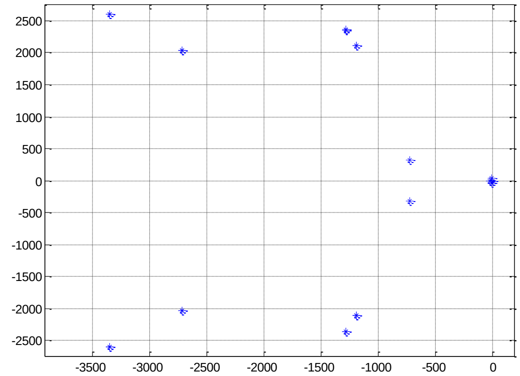

Fig. 4. Eigen values of the closed loop system.

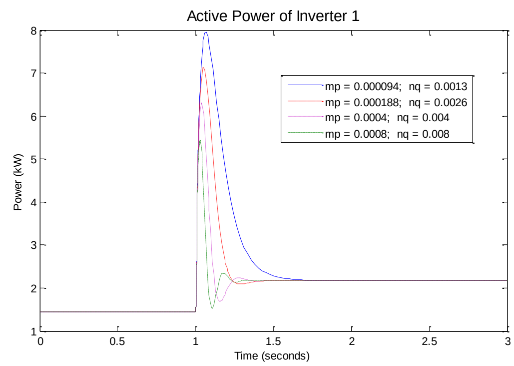

Fig. 5. Active power inverter 1 with droop variance

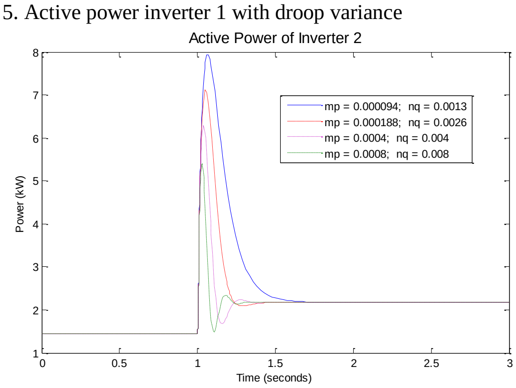

Fig. 6. Active power inverter 2 with droop variance

Figs. 5-6 show the fundamental active power sharing DG 1 and DG 2 for a 1.4 kW step change in load 1, respectively. In Fig. 5, it can be seen that before given load change at *t*=1s, initial active power at 1.4 kW. After given load change, inverter 1 gives active power 0.7 kW and, at t=1.5s, and it is steady at 2.1 kW. Similarly, in Fig. 6, it can be seen that, before the given load change at t=1s, initial active power at 1.4 kW. After load change is given, initial inverter 2 gives active power 0.7 kW and, at *t*=1.5s, and it is steady at 2.1 kW. Each inverter can

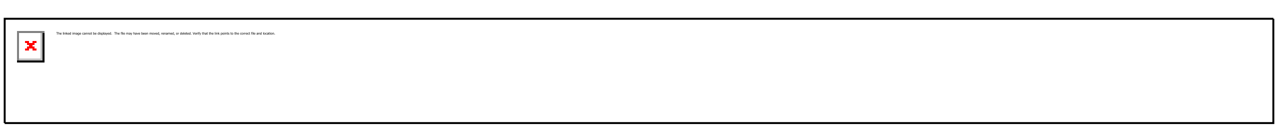

give power sharing half of need power demand 1.4 kW, inverter 1 gives 0.7 kW and also inverter 2 gives 0.7 kW.

Droop equation corresponds to active and reactive power. From Figs. 5-6, there are different transient responses of active power with droop variance. If droop constant is higher, overshoot of active power is lower, however it is faster to achieve the steady state condition. In other hand, if droop constant is lower, over shoot of active power is higher for the magnitude and the time constant is slower. With the same value of frequency, if the droop constant m_p increases then the overshoot of active power P decreases. Conversely, if the droop constant m_p decreases then the overshoot of active power P increases.

V. Conclusion

In this study, a small signal state space model of a microgrid was presented. The model included inverter, network, and load. All the sub-modules were individually modeled and were then combined to obtain the complete model of the microgrid of an AC single phase system. The model was analyzed in terms of the system eigenvalues to see the stability. Results obtained from the model showed the active power sharing among the inverters were able to occur. The results showed that the power of inverters were able to automatically follow the demand load power using the designed control.

References

[1] M. Kumar, S.N. Singh, and S.C. Srivastava, "Design and Control of Smart DC Microgrid for Integration of Renewable Energy Sources," *IEEE Proc. Elect. Eng,* 978-1-4673-2729, Sept. 2012.

[2] Nagaraju P., "Analysis, Control and Testing of Inverter-Based Distributed Generation in Standalone and Grid-Connected Applications," *Ph.D Thesis Imperial College*, London, UK, 2006.

[3] T. L. Vandoorn, B. Meersman, L. Degroote, B. Renders, and L. Vandevelde, "A control strategy for islanded microgrid swith DC-link voltage control*," IEEE Trans. Power Del.,* vol. 26, no. 2, pp. 703–713, Apr. 2011.

[4] Y. Mohamed and E. F. El-Saadany, "Adaptive decentralized droop controller to preserve power sharing stability of paralleled inverters in distributed generation microgrids," *IEEE Trans. Power Electron*., vol. 23, no. 6, pp. 2806–2816, Nov. 2008.

[5] I.-Y. Chung, W. Liu, D. A. Cartes, E. G. Collins, and S.-I. Moon, "Control methods of inverter-interfaced distributed generators in a microgrid system," *IEEE Trans. Ind. Appl*., vol. 46, no. 3, pp. 1078–1088, May/Jun. 2010.

[6] K. D. Brabandere, B. Bolsens, J. V. den Keybus, A.Woyte, J. Driesen, and R. Belmans, "A voltage and frequency droop control method for parallel inverters," *IEEE Trans. Power Electron*., vol. 22, no. 4, pp. 1107–1115, Jul. 2007.

[7] J. Kim, J. M. Guerrero, P. Rodriguez, R. Teodorescu, and K. Nam, "Mode adaptive droop control with virtual output impedances for an inverter-based flexible AC microgrid," *IEEE Trans. Power Electron*., vol. 26, no. 3, pp. 689–701, Mar. 2011.

[8] M. B. Delghavi and A. Yazdani, "An adaptive feedforward compensation for stability enhancement in droop-controlled inverter-based microgrids," *IEEE Trans. Power Del.,* vol. 26, no. 3, pp. 1764–1773, Jul. 2011.

[9] E. Barklund, N. Pogaku, M. Prodanovic, C. Hernandez-Aramburo, and T. C. Green, "Energy management in autonomous microgrid using stability-constrained droop control of inverters," *IEEE Trans. Power Electron*., vol. 23, no. 5, pp. 2346–2352, Aug. 2008.

[10] J. M. Guerrero, J. Matas, L. G. de Vicuña, M. Castilla, and J. Miret, "Decentralized control for parallel operation of distributed generation inverters using resistive output impedance," *IEEE Trans. Ind. Electron.*, vol. 54, no. 2, pp. 994–1004, Apr. 2007.

[11] P.C. Loh,D. Li, Y. K. Chai, and F. Blaabjerg, "HybridAC-DCmicrogrids with energy storages and progressive energy flow tuning," *IEEE Trans. Power Electron.*, vol. 28, no. 4, pp. 1533–1543, Apr. 2013.

[12] M. Kumar, S.C. Srivastava, and S.N. Singh "Dynamic Performance Analysis of DC Microgrid with a Proposed Control Strategy for Single-Phase VCVSI," IEEE Proc. Elect. Eng, 978-1-4799- 3656, April 2014.

[13] M. Prodanovic, T. Green, and H. Mansir, "A survey of control methods for parallel three-phase inverters connection," *Proc. Inst. Elect. Eng.*, no. 475, pp. 472–477, Sep. 2000.

[14] N. Pogaku, M. Prodanovic´, and T.C. Green, "Modeling, Analysis and Testing of AutonomousOperation of an Inverter-Based Microgrid," *IEEE Trans. on Power Electronics*, Vol. 22, No. 2, March 2007.

[15] J. M. Undrill, "Dynamic stability calculations for an arbitrary number of interconnected synchronous machines," *IEEE Trans. Power Apparat. Syst*., vol. PAS-87, no. 3, pp. 835–845, Mar. 1968.

[16] M. Prodanovic´, "Power Quality and Control Aspects of Parallel Connected Inverters in Distributed Generation," *Ph.D. dissertation, Imperial College,* Univ. London, London, UK, 2004.

[17] M. N. Marwali and A. Keyhani, "Control of distributed generation systems—Part I: voltages and current control," IEEE Trans. Power Electron., vol. 19, no. 6, pp. 1541–1550, Nov. 2004.R. J. Vidmar. (1992, August). On the use of atmospheric plasmas as electromagnetic reflectors. *IEEE Trans. Plasma Sci.* [Online]. *21(3).* pp. 876–880. Available: http://www.halcyon.com/pub/journals/21ps03-vidmar

S. Hadisupadmo received his B. Eng. in engineering physics from the Institut Teknologi Bandung, Indonesia, in 1977, Diplome from Universite in Energetique, Universite de Perpignan, France, in 1985,M. Eng. in instrumentation and control from the Institut Teknologi Bandung, Indonesia, in 1994, and Doctoral degree in engineering physics from the Institut Teknologi Bandung, Indonesia, in 2004. He works as a faculty member in engineering physics program in the faculty of industrial technology, Institut Teknologi Bandung, Indonesia.

His research interests include industrial process control and instrumentation, advanced process control, process control, adaptive estimation and control, system identification, optimal control, and power system control. He is a member of PII.

A. N. Hadiputro received his B. Eng in electrical engineering from the Institut Teknologi Sepuluh Nopember, Indonesia, in 2012 and M. Eng. in instrumentation and control from the Institut Teknologi Bandung, Indonesia, in 2015.

His research interests include power system control, modeling and simulation.

A. Widyotriatmo received his B. Eng. in engineering physics from the Institut Teknologi Bandung, Indonesia in 2002, M. Eng. in instrumentation and control from the Institut Teknologi Bandung, Indonesia, in 2006, and Ph.D. degree in mechanical engineering from Pusan National University, South Korea, in 2011. He joined the faculty of industrial technology as a faculty member for engineering physics program in the Institut Teknologi Bandung Indonesia in 2011.

His research interests include robotics, nonlinear control, energy optimization, control, and automation, biomedical instrumentation, metrology, process automation system, and power system control. He is a member of IEEE.